

# Combined Functional and Structural Evaluation of Cancer Patients with a Hybrid Camera–Based PET/CT System Using $^{18}\text{F}$ -FDG

Ora Israel, MD<sup>1,2</sup>; Maya Mor, MD<sup>1</sup>; Diana Gaitini, MD<sup>2,3</sup>; Zohar Keidar, MD<sup>1</sup>; Luda Guralnik, MD<sup>3</sup>; Ahuva Engel, MD<sup>2,3</sup>; Alex Frenkel, DSc<sup>1</sup>; Rachel Bar-Shalom, MD<sup>1</sup>; and Abraham Kuten, MD<sup>2,4</sup>

<sup>1</sup>Department of Nuclear Medicine, Rambam Medical Center, Haifa, Israel; <sup>2</sup>the B. Rappaport School of Medicine, Technion–Israel Institute of Technology, Haifa, Israel; <sup>3</sup>Department of Diagnostic Radiology, Rambam Medical Center, Haifa, Israel; and <sup>4</sup>Department of Oncology, Rambam Medical Center, Haifa, Israel

Correct diagnosis and definition of the functional and anatomic status of lesions in cancer patients are of clinical importance. The value of hybrid imaging using a gamma camera–based PET/CT and  $^{18}\text{F}$ -FDG in determining the relationship between mass and cancer was assessed. **Methods:** Hybrid imaging was performed using a device combining low-dose CT and gamma camera–based PET. Ninety-one patients with histologically proven malignancy and 190 suspected sites of disease were evaluated. Camera–based PET was performed after the injection of 296–370 MBq  $^{18}\text{F}$ -FDG. The presence of organomegaly or an abnormal mass on CT and of abnormal uptake of  $^{18}\text{F}$ -FDG was assessed for each suspected lesion. The presence of malignancy at each site was determined by biopsy, imaging follow-up, or clinical outcome. **Results:** Five imaging patterns were found. Pattern 1 showed congruent abnormal  $^{18}\text{F}$ -FDG uptake and a mass on CT in 110 of the lesions. One hundred two sites (93%) had active cancer. Pattern 2 showed a mass on CT, larger than the area of abnormal  $^{18}\text{F}$ -FDG uptake, and was found in 5 lesions. Active malignancy was proven in 3 sites (60%). Pattern 3 showed an abnormal mass on CT with no  $^{18}\text{F}$ -FDG uptake and was found in 52 lesions. Thirteen of these lesions (25%) had active tumor. Pattern 4 showing abnormal  $^{18}\text{F}$ -FDG uptake with no mass on CT was found in 23 lesions. Sixteen of these sites (70%) were malignant. Pattern 5 showed normal CT findings and no abnormal  $^{18}\text{F}$ -FDG uptake in 11 patients. Two of these patients (18%) had active disease. Hybrid imaging was of value in establishing the correct relationship between CT and  $^{18}\text{F}$ -FDG findings in 98 of the 190 lesions (52%). **Conclusion:** A range of patterns presenting with or without abnormal  $^{18}\text{F}$ -FDG uptake on camera–based PET and a mass on CT may occur in suspected cancer sites. Both structural changes on CT and increased cell metabolism expressed by abnormal  $^{18}\text{F}$ -FDG uptake should be considered in oncologic imaging. Hybrid imaging, a combined physiologic and anatomic modality, appears to provide new diagnostic opportunities in characterizing function and morphology in malignancies.

**Key Words:** tumor cell metabolism; camera–based PET; hybrid imaging

**J Nucl Med 2002; 43:1129–1136**

**I**maging plays a major role in the evaluation of cancer. Increase in size of normal organs, the presence of an abnormal mass, and changes in tissue attenuation are the main criteria for diagnosis of malignancy on CT (1). Clinical experience, however, shows that these criteria may be misleading, particularly after treatment (2,3). Nuclear medicine procedures, such as  $^{67}\text{Ga}$  scintigraphy and PET using  $^{18}\text{F}$ -FDG, have been used extensively to evaluate the functional characteristics of tumors and to monitor response to treatment in oncology (3–10). Intracellular  $^{18}\text{F}$ -FDG accumulation, due to trapping as a result of enhanced glucose metabolism in viable malignant cells, can be imaged using dedicated or gamma camera–based PET (8–12). However, nuclear medicine procedures in general and PET in particular lack anatomic landmarks for topographic orientation. Therefore, precise localization of sites of abnormal radio-tracer uptake may be difficult.

Registration of SPECT and PET with CT images has been described as a tool to provide good anatomic localization of functional data (13,14). Visual side-by-side analysis of nuclear medicine and CT studies are of value in characterizing large, single lesions as reported (15,16). Software-based coregistration of independently performed CT and scintigraphy is difficult to perform. Even with external fiducial markers, identical positioning of a patient when the procedures are done on 2 different devices may be inaccurate (2,17). As a rule, a patient lies with his hands above his head and holds his breath for the high-resolution CT study, which is a much shorter procedure than the nuclear medicine study. Also, the different computer matrices used for CT and PET and the need to manipulate the data to obtain

Received Sep. 5, 2001; revision accepted Apr. 26, 2002.

For correspondence or reprints contact: Ora Israel, MD, Department of Nuclear Medicine, Rambam Medical Center, Haifa, 35254 Israel.  
E-mail: o\_israel@rambam.health.gov.il

fusion images are problematic. These techniques have, therefore, not reached routine clinical use, except for rigid regions of the body, such as the head. Discrepancies that may be detected on fused images between the presence and location of a tumor mass on CT and that of abnormal radiotracer uptake either may be attributed to drawbacks of the registration technique or may represent true findings.

This dilemma is overcome when imaging of both modalities is done in a single session, using the same gantry, stretcher, and software. A hybrid device combining a dual-head, variable-angle gamma camera with coincidence acquisition capabilities and a low-dose x-ray system has been recently introduced (18–20). This new imaging concept was initially developed to provide CT numbers for attenuation correction of the 511-keV positron annihilation radiation of  $^{18}\text{F}$ -FDG. By generating low-resolution CT images, this combined technique also allows correct coregistration of anatomic and functional data. Simultaneously obtained hybrid images provide the technical framework for precise localization of the metabolically active focus detected on camera-based  $^{18}\text{F}$ -FDG PET and for defining the functional status of lesions detected on CT.

This study describes the initial experience in 91 patients with known malignancies using transmission emission tomography (TET) obtained with the hybrid camera-based PET/CT device using  $^{18}\text{F}$ -FDG in evaluating the relationship between tumor mass and cancer in 190 sites suspected of malignancy. This relationship has been validated in a tumor model (21) and suggested in lymphoma patients (5–7,22–24).

## MATERIALS AND METHODS

### Hybrid Camera-Based PET/CT Imaging Protocol

The studies were performed using a combined transmission and emission device installed on the same gantry. A nuclear medicine dual-detector, variable-angle gamma camera system with coincidence acquisition capabilities and an x-ray tube and detector that produce cross-sectional anatomic CT images are both placed on the rotating support of the gamma camera (Millennium VG & Hawkey; General Electric Medical Systems, Milwaukee, WI). Nuclear medicine and CT images are acquired serially on the same gantry. The sequence of transmission and emission acquisition is interchangeable; either modality can be acquired first. Continuous rotation of the x-ray system and the nuclear medicine detectors is performed using the slip ring technique.  $^{18}\text{F}$ -FDG imaging is initiated 60 min after the intravenous injection of 296–370 MBq (8–10 mCi)  $^{18}\text{F}$ -FDG. Coincidence data are acquired for 10 rotations of 360° over a period of 30 min. A dual window technique is used, accepting coincidence between photopeak events and between photopeak and Compton events. The acquisition matrix is 128 × 128. The data are rebinned into 90 projections and reconstructed iteratively including attenuation correction. Iterative reconstruction is performed using COSEM (Coincidence Ordered Subsets Expectation Maximization; 8 subsets, 2 steps), a software package provided by the manufacturer (General Electric Medical Systems). The x-ray attenuation measurements are acquired as part of the camera acquisition protocol. The x-ray tube is a fixed anode, oil-cooled tube operated at 140 kV, 2.5 mA. The rotation speed at

the time of acquisition is of 2.6 revolutions per minute. A half-scan acquisition is performed over 216° with 14-s acquisition time for each slice. The transmission measurements taken through the patient are corrected and logged to produce attenuation measurements. The attenuation map is used to correct for the attenuation of the 511-keV  $\gamma$ -rays. The x-ray images are capable of 1-mm resolution, but the localization images are produced on a 4-mm pixel size, similar to the nuclear medicine images. The low-contrast performance is specified as detecting 3-mm-diameter rods with 2.5% contrast in a 20-cm-diameter phantom. The x-ray images are reconstructed onto a 256 × 256 matrix and readjusted to match the scale of the emission reconstruction. The x-ray reconstructed image is implemented into the nuclear medicine database together with the nuclear medicine data (Entegra; General Electric Medical Systems). Matching pairs of  $^{18}\text{F}$ -FDG and x-ray slices are fused and an image overlaying the  $^{18}\text{F}$ -FDG activity on the corresponding anatomic plane is generated.

### Patient Population

One hundred four consecutive patients with histologically proven malignancies referred for camera-based  $^{18}\text{F}$ -FDG PET had hybrid imaging. The Institutional Ethics Committee approved the study. The files of 13 patients lacked further clinical information on the status of disease, and these patients were excluded from the study. Therefore, the final study population included 91 patients with 190 suspected sites of disease (60 male, 31 female patients; mean age, 49 y; range, 8–84 y). Clinical information is summarized in Table 1. The presence or absence of active malignancy was histologically proven by fine-needle aspiration, excisional biopsy, or pathologic examination after surgery in 30 patients. In 52 patients the final diagnosis was determined by changes in the size or pattern of suspected lesions on follow-up imaging studies and in 9 patients with negative studies by clinical outcome. Patients with no further evidence of disease had a mean period of clinical and radiologic follow-up of 12 mo (range, 9–17 mo). Both malignant and benign lesions could be found in individual patients with multiple suspected sites. A final diagnosis of the malignant or benign etiology was established for each of the lesions in each patient.

The criteria for interpretation of camera-based  $^{18}\text{F}$ -FDG PET studies included the presence of abnormally increased tracer uptake at each suspected site. CT criteria for malignancy included the presence of organomegaly, of an abnormal mass, or of structural

**TABLE 1**  
Clinical Data in 91 Patients Evaluated with Hybrid  
Camera-Based PET/CT Device

Parameter	Lung Lymphoma	Lung cancer	GIT tumors	Other tumors
No. of patients	36	23	14	18
No. of sites	93	41	18	38
TET at staging (no. of patients)	5	6	—	—
TET at end of treatment (no. of patients)	16	5	3	2
TET in suspected recurrence (no. of patients)	15	12	11	16

GIT = gastrointestinal tumors.

changes inside a normal-sized organ. Fifty-three lesions (28%) had a diameter of  $\leq 15$  mm, whereas 93 lesions (49%) were  $>15$  mm in diameter. The size of 44 sites could not be measured precisely because of their location or CT characteristics. The low-resolution CT images of the combined studies performed without injection of contrast agents were used for localization of lesions and for comparison with high-resolution, contrast-enhanced CT studies, viewed at the same anatomic level in all patients. Size of lesions was assessed using a 2-dimensional method on high-resolution conventional CT. Two diameters were measured in the representative slices that best visualized the lesion.

### Data Analysis

Three experienced nuclear medicine physicians interpreted camera-based  $^{18}\text{F}$ -FDG PET studies. High-resolution, contrast-enhanced CT studies were interpreted by 3 experienced radiologists. In case of disagreement the final interpretation was determined by a majority opinion for both nuclear medicine and CT. Radiologists and nuclear medicine physicians interpreted the high-resolution CT and camera-based  $^{18}\text{F}$ -FDG PET with knowledge of the medical history of the patient. They were unaware of the results of the other imaging modality. Nuclear medicine physicians and radiologists interpreted hybrid images together. Hybrid imaging patterns were defined for each site of disease according to the presence or absence of findings in each of the 2 modalities. A pattern showing abnormal findings on either CT or PET, or both modalities, in a malignant lesion was considered a true-positive (TP) result. A pattern showing abnormalities on either 1 or both modalities, when malignancy was not proven, was considered a false-positive (FP) result. In patients with multiple suspected lesions, different patterns could be seen in different sites and the presence or absence of active malignancy was recorded for each suspected lesion.

TET was considered of value for establishing the pattern at an evaluated site when the hybrid images allowed for retrospective lesion detection on high-resolution CT or led to precise localization of abnormal  $^{18}\text{F}$ -FDG uptake. Criteria for precise localization of abnormal  $^{18}\text{F}$ -FDG uptake included determining the presence of increased activity in each of multiple lesions located in close vicinity on CT, allowing for the differential diagnosis of uptake as being caused by physiologic  $^{18}\text{F}$ -FDG activity or related to disease and providing the exact topographic coordinates of abnormal  $^{18}\text{F}$ -FDG uptake either inside a larger lesion seen on CT or in a patient with a negative CT study.

### RESULTS

Ninety-one patients with 190 lesions were evaluated. Ten lesions were located in the neck, 120 lesions were in the chest, 39 lesions were in the abdomen, and 21 lesions were in the pelvis. There was a mean of 2 lesions per patient (range, 0–14). Twenty-nine patients had a single lesion. One hundred thirty-four lesions were subsequently proven to be malignant. Fifty-six sites had no further proof of malignancy. Five patterns of findings were found on hybrid TET images.

Pattern 1 showed the presence of a mass on CT and abnormal  $^{18}\text{F}$ -FDG uptake of the same size. This was found in 110 lesions (58%) (Fig. 1). This congruent pattern was TP for the presence of active cancer in 102 lesions (93%). Eleven of these lesions had a diameter of  $\leq 15$  mm. Of the 102 TP lesions with pattern 1, there were 23 primary tumors at staging, 30 metastases, 13 residual tumors after treatment, and 36 sites of recurrence. In 8 sites (7%) there was no

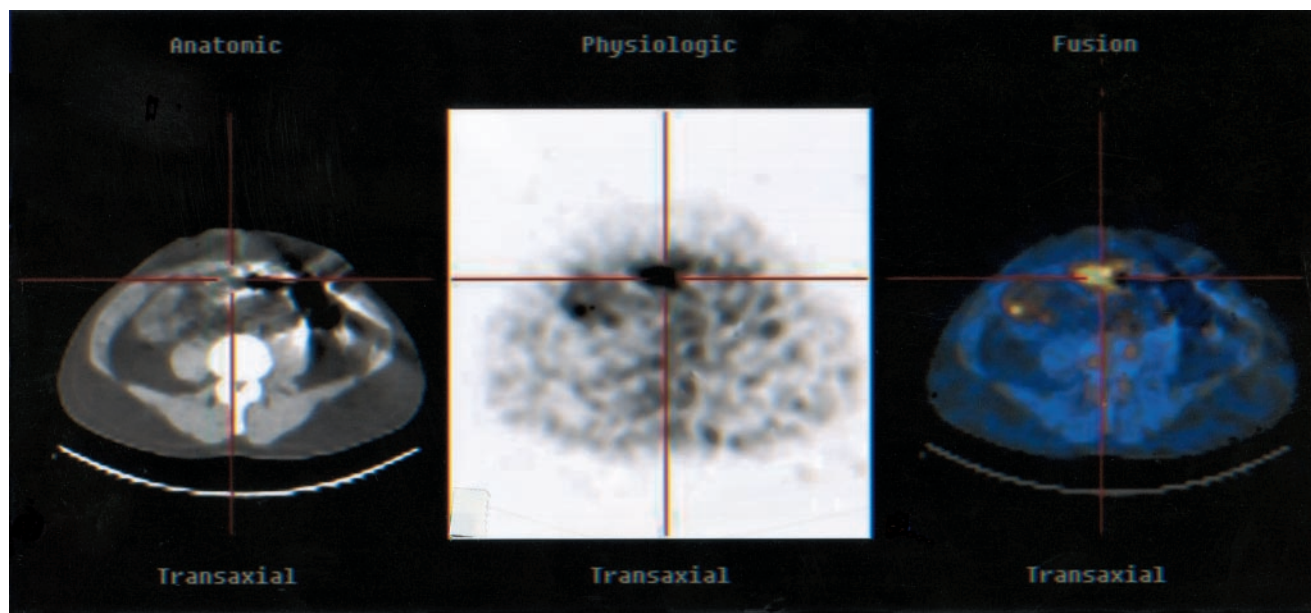


**FIGURE 1.** Pattern 1: congruent findings of abnormal  $^{18}\text{F}$ -FDG uptake and mass on CT in recurrent colon cancer. A 31-y-old male patient with adenocarcinoma of cecum, Duke's stage C2, state after right hemicolectomy. There is thickening of intestinal wall at level of anastomosis on CT (left) with abnormal  $^{18}\text{F}$ -FDG uptake (center) of similar size and location as confirmed by hybrid TET (right) images. Red markers are used for exact localization of lesion on all components of hybrid study. Surgery confirmed recurrence at site of anastomosis.

further evidence for active malignancy. Two of these lesions had a diameter of  $\leq 15$  mm. Six of the FP sites showed treatment-related inflammatory changes and 2 represented thymic hyperplasia. Hybrid TET images were of value in correctly defining pattern 1 in 70 lesions. In 57 lesions it allowed for the exact localization of the abnormal  $^{18}\text{F}$ -FDG uptake. In 13 sites it allowed for retrospective lesion detection on CT.

Pattern 2 showed an abnormal mass on CT that was larger than the area of increased  $^{18}\text{F}$ -FDG uptake. This pattern was defined visually when hybrid images showed a difference between the anatomic borders of a lesion on CT and the area of increased  $^{18}\text{F}$ -FDG uptake localized only to a part of the mass. Pattern 2 was seen in 5 lesions (3%) (Fig. 2). All lesions were  $>15$  mm in diameter. Pattern 2 was TP for the presence of active malignancy in 3 lesions (60%): 2 sites of residual cancer and 1 recurrence in a residual mass after treatment. The 2 FP lesions represented severe inflammatory changes after radiation. Hybrid TET images were of value in correctly defining pattern 2 in all lesions. Hybrid imaging determined the precise relationship between the size of the lesion on both modalities and the exact localization of the abnormal  $^{18}\text{F}$ -FDG uptake inside the mass seen on CT.

Pattern 3 showed an abnormal mass on CT with no  $^{18}\text{F}$ -FDG uptake. This was seen in 52 sites (27%) (Fig. 3). This pattern was TP for active cancer in 13 lesions (25%). Twelve of these lesions had a diameter of  $\leq 15$  mm. Pattern 3 was TP in 5 primary tumors at staging, 5 metastases, and 3 residual tumors after treatment. Pattern 3 was found in 39

lesions with no further evidence for malignancy: 26 residual masses with no further evidence of viable tumor, 7 sites of inflammatory changes, 4 enlarged lymph nodes at staging in which malignancy was not found during surgery, and 2 sites of technical artifacts on CT. Twenty-eight of these lesions had a diameter of  $\leq 15$  mm.

Pattern 4 showed abnormal  $^{18}\text{F}$ -FDG uptake with no abnormal findings on high-resolution CT with no image degradation due to artifacts. This pattern was found in 23 sites (12%) (Fig. 4). Pattern 4 was TP for the presence of cancer in 16 lesions (70%): 11 metastases and 5 sites of recurrence. In 7 lesions there was no evidence of malignancy. Four of these FP lesions were further diagnosed as inflammatory changes, and there was 1 case of thymus hyperplasia. In 2 sites of increased  $^{18}\text{F}$ -FDG uptake, malignancy was not confirmed during follow-up, and the reason for the abnormal  $^{18}\text{F}$ -FDG findings remains unknown. The time elapsed between the high-resolution CT and the camera-based PET/CT study was a mean of  $30 \pm 17$  d for both TP and FP lesions. Hybrid TET images were of value in all lesions presenting with pattern 4, providing the topographic landmarks for correct localization of abnormal  $^{18}\text{F}$ -FDG uptake and, therefore, guiding further diagnostic procedures.

Pattern 5 showed negative CT and  $^{18}\text{F}$ -FDG studies and was present in 11 patients. Nine of these patients (82%) had no evidence of disease. The 2 false-negative studies included 1 patient with lymphoma of the bone marrow and 1 patient with a mixed small- and large-cell non-Hodgkin's lymphoma of the skin presenting with a tumor located on

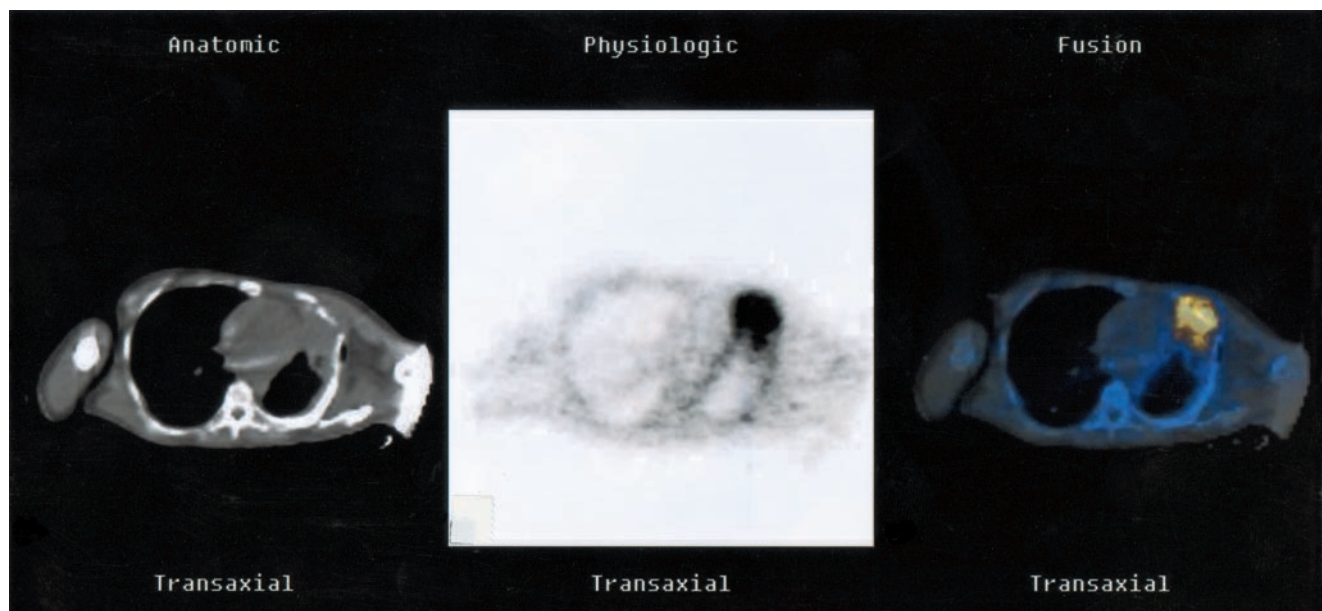


**FIGURE 2.** Pattern 2: incongruent findings of abnormal  $^{18}\text{F}$ -FDG uptake representing residual cancer inside larger residual mass seen on CT after treatment. A 34-y-old male patient with leiomyosarcoma of left chest wall. There was decrease in size of tumor on repeated CT studies after chemo- and radiotherapy, suggesting response to treatment. However, CT (left),  $^{18}\text{F}$ -FDG (center), and hybrid TET (right) images indicate presence of viable cancer inside residual tumor mass. Patient died with tumor progression 6 wk later.

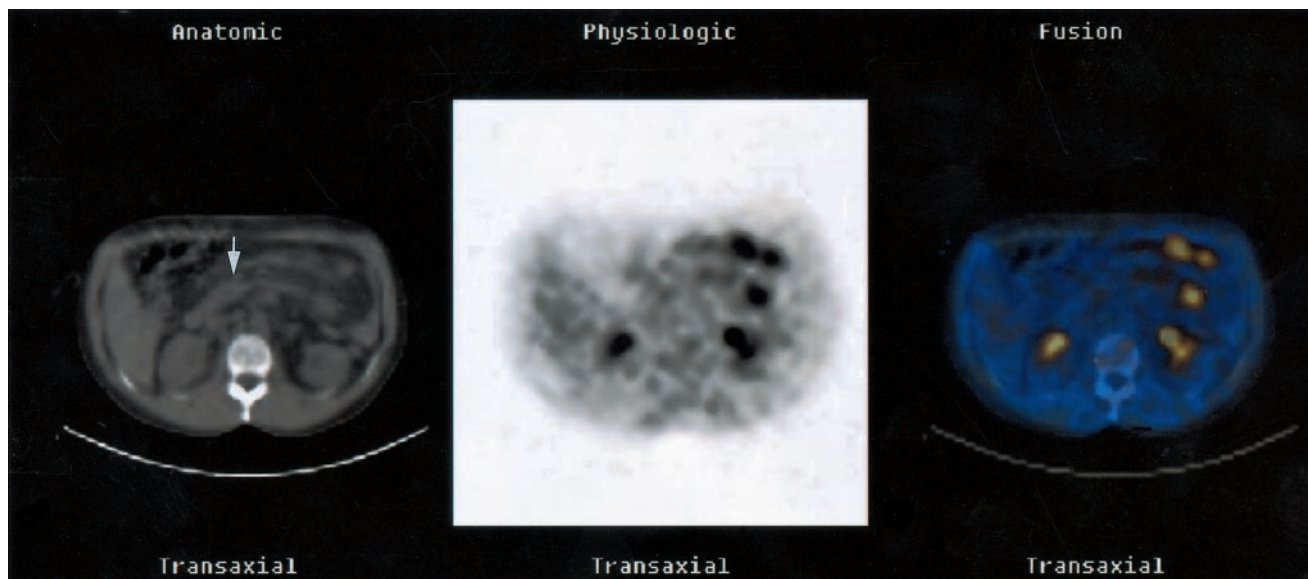


**FIGURE 3.** Pattern 3: incongruent findings of residual mass on CT with no  $^{18}\text{F}$ -FDG uptake indicating no viable cancer. A 49-y-old female patient with recurrent abdominal low-grade non-Hodgkin's lymphoma, state after chemo- and radiotherapy. CT image (left) shows mild-to-moderate mesenteric lymphadenopathy (arrow). There is no abnormal  $^{18}\text{F}$ -FDG uptake (center) in same localization as shown on hybrid TET image (right). TET also localizes increased  $^{18}\text{F}$ -FDG uptake in left abdomen to physiologic colon excretion. Patient has been in continuous clinical remission for >14 mo.

the back, 15 mm in diameter. In these 2 false-negative studies, attenuation-corrected and uncorrected  $^{18}\text{F}$ -FDG images were reviewed and showed no abnormalities.

Incongruent metabolic and morphologic findings, patterns 2–4, were found in 80 lesions (42%). Hybrid TET images were of value in establishing the pattern of functional and anatomic characteristics in 98 of the 190 suspected lesions (52%). The relationship between camera-based PET/CT patterns and the presence of active cancer is summarized in Table 2.

## DISCUSSION

CT is considered the modality of choice for evaluation of patients with malignancy, based on the detection of an abnormal mass or enlargement of organs, usually lymph nodes, caused by cancer growth (1,3). The role of PET using  $^{18}\text{F}$ -FDG in the evaluation of cancer is based on the increased glucose use by malignant cells compared with that of normal tissue (8–10).

Findings determining the presence of tumor are not always congruent on these 2 imaging modalities. The term “unexpected N2 disease” (metastatic mediastinal lymph nodes of normal size) in non-small cell lung cancer was introduced following the clinical observation that malignancy may not always be associated with lymphadenopathy. There may be a significant overlap between the diameter of malignant and benign nodes (25,26). After treatment, there may also be a discrepancy between the presence of a residual mass and that of residual viable cancer (21,27). In an animal tumor model, no linear relationship between uptake of tritiated deoxyglucose and size of treated tumors was

found (21). The term “unconfirmed complete response” reflects the clinical dilemma related to the presence of a residual mass in up to 50% of treated lymphoma patients in the absence of active malignancy (28). Because functional changes may precede morphologic findings, relapse of lymphoma can be diagnosed by  $^{67}\text{Ga}$  or  $^{18}\text{F}$ -FDG PET months and even years before a mass can be palpated or seen on CT (29,30). Nevertheless, for the lack of better criteria, efforts to standardize the definition of response to treatment still rely in part on measuring and comparing the size of lesions (29).

This report presents preliminary results on the value of hybrid imaging in detecting and correctly defining the functional and anatomic imaging characteristics in cancer patients. It shows the wide range of CT and  $^{18}\text{F}$ -FDG PET combined patterns and emphasizes the potential use of hybrid images in differentiating between the presence of a mass and that of viable cancer. Hybrid imaging improves the assessment of the true relationship between the size and function of a suspected lesion. With the use of camera-based PET/CT, acquisition of  $^{18}\text{F}$ -FDG and low-dose CT are both performed during normal breathing. Differences in patient positioning due to motion between the 2 sequences of the combined study are less likely to occur and, therefore, correct coregistration is not a technical challenge. The feasibility of hybrid imaging in terms of its ability to accurately register PET and CT in the torso has been validated by previous studies (18–20).

Single-session, sequential, imaging of tumor mass and tumor metabolism improves the understanding of imaging neoplasms (5,6,24,26). In this study population, hybrid im-

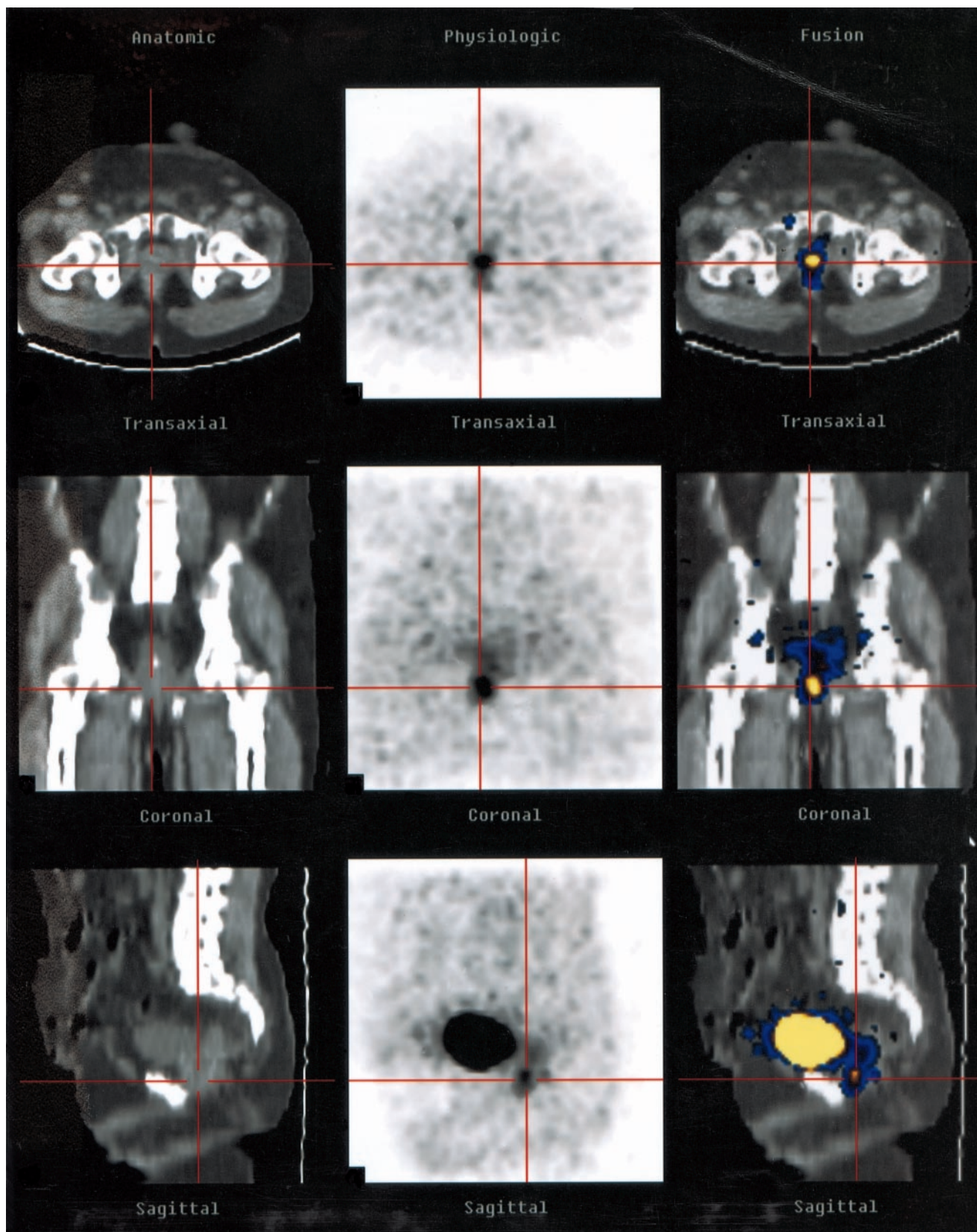


**TABLE 2**  
Relationship Between Hybrid Imaging TET Patterns  
of Tumor Mass and Cancer in 80 Patients and  
190 Sites with Suspected Malignancy

TET pattern	Total no. of sites	TP lesions*		FP lesions†	
		No.	%	No.	%
1. CT+ = FDG+	110	102	93	8	7
2. CT+ > FDG+	5	3	60	2	40
3. CT+, FDG-	52	13	25	39	75
4. CT-, FDG+	23	16	70	7	30

\*TP lesions: sites with proven active cancer.

†FP lesions: sites with no further evidence of malignancy.

Eleven patients with negative CT and camera-based PET study (pattern 5) presented in Results are not included in table.

ages defined the precise anatomic localization and characterization of the functional status of 52% of the suspected sites, either by better localization of abnormal  $^{18}\text{F}$ -FDG uptake or by pinpointing to a previously missed lesion on CT.

In patients with known malignancies a mass does not necessarily contain only neoplastic tissue. A mass shrinking in size on repeated CT studies, considered a criterion of response to treatment, can, however, still contain a significant amount of viable cancer tissue. Hybrid TET images, as in pattern 2, provide this important clinical information (Fig. 2). As defined by pattern 3, cancer may be present in a mass detected by CT without abnormal  $^{18}\text{F}$ -FDG uptake on camera-based PET. Because this pattern was found in 23% of small lesions, at present a negative camera-based PET acquisition is suggestive of the absence of disease in sites with a diameter of  $\geq 15$  mm. Technical improvements in hardware, better software options, and fusion protocols, leading to a higher lesion detectability on camera-based and dedicated PET imaging, will decrease, in the future, the incidence of small malignant lesions presenting with pattern 3 on hybrid imaging. In patients with no evidence of disease, pattern 3 increased the level of confidence in the final decision-making that a residual mass does not show any abnormal  $^{18}\text{F}$ -FDG uptake and that the patient has achieved a complete response.

Hybrid TET imaging improves the inherent value of nuclear medicine procedures for early diagnosis of metastases and relapse. It shows the existence and exact localization of a previously unsuspected malignant focus presenting

as pattern 4, characterized only by the presence of abnormal  $^{18}\text{F}$ -FDG uptake (Fig. 4). Although pattern 4 was less common than pattern 3 in this study, 70% of lesions showing only increased  $^{18}\text{F}$ -FDG uptake without a mass were malignant compared with only 25% of sites that showed an abnormal mass with no  $^{18}\text{F}$ -FDG uptake. By correctly localizing and defining areas of increased  $^{18}\text{F}$ -FDG uptake as unrelated to cancer, hybrid imaging also leads to a decrease in the rate of FP results and improves the specificity of  $^{18}\text{F}$ -FDG PET.

TET may potentially decrease the incidence of sampling error related to biopsy. When increased  $^{18}\text{F}$ -FDG uptake is the sole indicator of cancer at staging or early during relapse, as described by pattern 4, its precise localization provided by hybrid imaging is of value for further radiologic evaluation and for histologic sampling. Precise localization of viable cancer inside a larger mass in lesions presenting as pattern 2 may be also used for guiding procedures aiming for tissue diagnosis. Histologic samples should be obtained from the cancer and not from a fibrotic or necrotic part of the mass.

The finding of a dissociation between the presence of a mass and the existence of cancer is important because it may alter clinical management of cancer patients. The ability of hybrid TET images to accurately localize a hypermetabolic viable tumor focus results in a change in the radiologic and oncologic criteria for staging and restaging of cancer, which may potentially lead to better diagnosis and improve the therapeutic approach. In the future, hybrid imaging will play a role in radiotherapy and brachytherapy planning to the part of the tumor containing viable malignant cells rather than aiming to the entire mass.

This preliminary report describes hybrid imaging patterns in a large variety of histologic tumor types. Further studies are necessary to assess the value of hybrid imaging in specific neoplasms, at staging and during follow-up, in specific anatomic regions and to compare the incremental value of the combined approach to single imaging modalities or coregistration of separately performed studies. A few additional issues related to hybrid imaging devices still await their solution. The benefit-to-risk ratio of additional radiation to patients, the incremental cost of a combined instrument, and the performance level of PET and CT that should be used in this type of apparatus still need to be evaluated. Guidelines for patient referral to hybrid imaging need to be developed.

**FIGURE 4.** Pattern 4: incongruent findings of abnormal  $^{18}\text{F}$ -FDG uptake indicating presence of active cancer with no mass on CT. A 59-y-old male patient, 4 y after abdominoperineal resection for well-differentiated cancer of rectum, stage C2, and elevated levels of tumor serum markers.  $^{18}\text{F}$ -FDG images (center) show abnormal uptake localized by hybrid TET images (right) to prostate, which is of normal size on CT image (left). Studies are presented in transaxial (top row), coronal (middle row), and sagittal (bottom row) planes. Red markers are used to allow for exact localization of lesion on CT. Biopsy was guided by precise localization provided by hybrid imaging. It revealed metastasis from rectal cancer to prostate, detected by abnormal  $^{18}\text{F}$ -FDG uptake but not by CT.

## CONCLUSION

Hybrid TET imaging shows the presence of a mass, assesses whether the mass contains cancer, and identifies the precise localization of viable malignant cells inside an anatomic lesion. Fused studies also show that early cancer can be present as a hypermetabolic area in the absence of an anatomically defined lesion. Hybrid imaging of tumor metabolism by  $^{18}\text{F}$ -FDG PET and tumor size and topography by CT appears to be an important clinical tool in the evaluation and management of cancer patients to be further assessed in larger, more homogeneous groups of patients.

## ACKNOWLEDGMENTS

This work is dedicated to the vision, teaching, and leadership of Dr. Dov Front. The authors thank Drs. Gerald M. Kolodny and Stanley J. Goldsmith for their useful suggestions in preparing the manuscript. This work was supported in part by a grant from the L. Rosenblatt Fund of the Technion Foundation for Research in Cancer and by a research grant from Elgems, Ltd. (Haifa, Israel).

## REFERENCES

- Castellino RA, Hilton S, O'Brien P, et al. Non-Hodgkin lymphoma: contribution of chest CT in the initial staging solution. *Radiology*. 1996;199:129–132.
- Berlangieri SU, Scott AM. Metabolic staging of lung cancer. *N Engl J Med*. 2000;343:290–292.
- Hopper KD, Singapur K, Finkel A. Body CT and oncologic imaging. *Radiology*. 2000;215:27–40.
- Front D, Israel O. Nuclear medicine in monitoring response to cancer treatment [editorial]. *J Nucl Med*. 1989;30:1731–1736.
- Israel O, Front D, Lam M, et al. Gallium-67 imaging in monitoring lymphoma response to treatment. *Cancer*. 1988;61:2439–2443.
- Front D, Ben Haim S, Israel O, et al. Lymphoma: predictive value of Ga-67 scintigraphy after treatment. *Radiology*. 1992;182:359–363.
- Front D, Bar-Shalom R, Israel O. The continuing clinical role of Ga-67 scintigraphy in the age of receptor imaging. *Semin Nucl Med*. 1997;27:68–74.
- Wahl RL, Hutchins GD, Buchsbaum DJ, et al.  $^{18}\text{F}$ -2-Deoxy-2-fluoro-D-glucose uptake into human tumor xenografts: feasibility studies for cancer imaging with positron emission tomography. *Cancer*. 1991;67:1544–1550.
- Strauss LG, Conti PS. The application of PET in clinical oncology. *J Nucl Med*. 1991;32:623–648.
- Bar-Shalom R, Valdivia AY, Blaufox MD. PET imaging in oncology. *Semin Nucl Med*. 2000;30:150–185.
- MacFarlane DJ, Cotton L, Ackerman RJ, et al. Triple-head SPECT with 2-[fluorine-18]fluoro-deoxy-D-glucose (FDG): initial evaluation in oncology and comparison with FDG PET. *Radiology*. 1995;194:425–429.
- Delbeke D, Patton JA, Martin WH, Sandler MP. FDG PET and dual-head gamma camera positron coincidence detection imaging of suspected malignancies and brain disorders. *J Nucl Med*. 1999;40:110–117.
- Weber DA, Ivanovic M. Correlative image registration. *Semin Nucl Med*. 1994;24:311–323.
- Wahl RL, Quint LE, Cieslak RD, et al. "Anatomometabolic" tumor imaging: fusion of FDG PET with CT or MRI to localize foci of increased activity. *J Nucl Med*. 1993;34:1190–1197.
- Correia JA. Registration of nuclear medicine images. *J Nucl Med*. 1990;31:1227–1229.
- Shreve PD. Adding structure to function. *J Nucl Med*. 2000;41:1380–1382.
- Wahl RL, Quint LE, Greenough RL, et al. Staging of mediastinal non-small cell lung cancer with FDG PET, CT and fusion images: preliminary prospective evaluation. *Radiology*. 1994;191:371–377.
- Bocher M, Balan A, Krausz Y, et al. Gamma camera-mounted anatomical x-ray tomography: technology, system characteristics and first images. *Eur J Nucl Med*. 2000;27:619–627.
- Patton JA, Delbeke D, Sandler MP. Image fusion using an integrated, dual-head coincidence camera with x-ray tube-based attenuation maps. *J Nucl Med*. 2000;41:1364–1368.
- Delbeke D, Martin WH, Patton JA, et al. Value of iterative reconstruction, attenuation correction and image fusion in the interpretation of FDG PET images with an integrated dual-head coincidence camera and x-ray based attenuation maps. *Radiology*. 2001;218:163–171.
- Iosilevsky G, Front D, Bettman L, et al. Uptake of gallium-67 citrate and [2- $^3\text{H}$ ]deoxyglucose in a tumor model, following chemotherapy and radiotherapy. *J Nucl Med*. 1985;26:278–282.
- Kaplan WD, Jochelson MS, Herman TS, et al. Gallium-67 imaging: a predictor of residual tumor viability and clinical outcome in patients with diffuse large-cell lymphomas. *J Clin Oncol*. 1990;8:1966–1970.
- Front D, Bar-Shalom R, Mor M, et al. Hodgkin disease: prediction of outcome with Ga-67 scintigraphy after one cycle of chemotherapy. *Radiology*. 1999;210:487–491.
- Front D, Bar-Shalom R, Mor M, et al. Aggressive non-Hodgkin lymphoma: early prediction of outcome with Ga-67 scintigraphy. *Radiology*. 2000;214:253–257.
- Goldstraw P, Mannan GM, Kaplan D, et al. Surgical management of non small cell lung cancer with mediastinal node metastases (N2 disease). *J Thorac Cardiovasc Surg*. 1994;107:19–28.
- Arita T, Mastumoto T, Kuramitsu T, et al. Is it possible to differentiate malignant mediastinal nodes from benign nodes by size? *Chest*. 1996;110:1004–1008.
- Canellos GP. Residual mass may not be residual cancer [editorial]. *J Clin Oncol*. 1988;6:931–933.
- Cheson BD, Horning SJ, Coiffier B, et al. Report of an international workshop to standardize response criteria for non-Hodgkin's lymphomas. *J Clin Oncol*. 1999;17:1244–1253.
- Front D, Bar-Shalom R, Epelbaum R, et al. Early detection of lymphoma recurrence with gallium-67 scintigraphy. *J Nucl Med*. 1993;34:2101–2104.
- Spaepen K, Stroobants S, Dupont P, et al. Prognostic value of positron emission tomography (PET) with fluorine-18 fluorodeoxyglucose ( $^{18}\text{F}$ FDG) after first-line chemotherapy in non-Hodgkin's lymphoma: Is  $^{18}\text{F}$ FDG-PET a valid alternative to conventional diagnostic methods? *J Clin Oncol*. 2001;19:414–419.



The Journal of  
NUCLEAR MEDICINE

## Combined Functional and Structural Evaluation of Cancer Patients with a Hybrid Camera-Based PET/CT System Using $^{18}\text{F}$ -FDG

Ora Israel, Maya Mor, Diana Gaitini, Zohar Keidar, Luda Guralnik, Ahuva Engel, Alex Frenkel, Rachel Bar-Shalom and Abraham Kuten

*J Nucl Med.* 2002;43:1129-1136.

---

This article and updated information are available at:  
<http://jnm.snmjournals.org/content/43/9/1129>

---

Information about reproducing figures, tables, or other portions of this article can be found online at:  
<http://jnm.snmjournals.org/site/misc/permission.xhtml>

Information about subscriptions to JNM can be found at:  
<http://jnm.snmjournals.org/site/subscriptions/online.xhtml>

*The Journal of Nuclear Medicine* is published monthly.  
SNMMI | Society of Nuclear Medicine and Molecular Imaging  
1850 Samuel Morse Drive, Reston, VA 20190.  
(Print ISSN: 0161-5505, Online ISSN: 2159-662X)

© Copyright 2002 SNMMI; all rights reserved.